



Comparative study of serine-plasmalogens in human retina and optic nerve: identification of atypical species with odd carbon chains

Kornél Nagy, Viral Vishnuprasad Brahmbhatt, Olivier Berdeaux, Lionel Brétillon, Frédéric Destailats, Niyazi Acar

► To cite this version:

Kornél Nagy, Viral Vishnuprasad Brahmbhatt, Olivier Berdeaux, Lionel Brétillon, Frédéric Destailats, et al.. Comparative study of serine-plasmalogens in human retina and optic nerve: identification of atypical species with odd carbon chains. *Journal of Lipid Research*, 2012, 53 (2012), pp.776-783. 10.1194/jlr.D022962 . hal-02644230

HAL Id: hal-02644230

<https://hal.inrae.fr/hal-02644230>

Submitted on 28 May 2020

HAL is a multi-disciplinary open access archive for the deposit and dissemination of scientific research documents, whether they are published or not. The documents may come from teaching and research institutions in France or abroad, or from public or private research centers.

L'archive ouverte pluridisciplinaire **HAL**, est destinée au dépôt et à la diffusion de documents scientifiques de niveau recherche, publiés ou non, émanant des établissements d'enseignement et de recherche français ou étrangers, des laboratoires publics ou privés.

Copyright

Comparative study of serine-plasmalogens in human retina and optic nerve: identification of atypical species with odd carbon chains

Kornél Nagy,* Viral Vishnuprasad Brahmabhatt,* Olivier Berdeaux,[†] Lionel Bretillon,[§] Frédéric Destailhats,^{1,*} and Niyazi Acar[§]

Nestlé Research Center,* Vers-chez-les-Blanc, Lausanne, Switzerland; Chemosens Platform,[†] and Eye and Nutrition Research Group,[§] Centre des Sciences du Goût et de l'Alimentation, UMR6265 CNRS, UMR 1324 INRA, Université de Bourgogne, F-21000 Dijon, France

Abstract The objective of this work was to detect and identify phosphatidylserine plasmalogen species in human ocular neurons represented by the retina and the optic nerve. Plasmalogens (vinyl-ether bearing phospholipids) are commonly found in the forms of phosphatidylcholine and phosphatidylethanolamine in numerous mammalian cell types, including the retina. Although their biological functions are unclear, the alteration of cellular plasmalogen content has been associated with several human disorders such as rhizomelic chondrodysplasia punctata Type 2 and primary open-angle glaucoma. By using liquid chromatography coupled to high-resolution and tandem mass spectrometry, we have identified for the first time several species of phosphatidylserine plasmalogens, including atypical forms having moieties with odd numbers of carbons and unsaturation in *sn*-2 position. Structural elucidation of the potential phosphatidylserine ether linked species was pursued by performing MS³ experiments, and three fragments are proposed as marker ions to deduce which fatty acid is linked as ether or ester on the glycerol backbone. Interpretation of the fragmentation patterns based on this scheme enabled the assignment of structures to the *m/z* values, thereby identifying the phosphatidylserine plasmalogens.—Nagy, K., V. V. Brahmabhatt, O. Berdeaux, L. Bretillon, F. Destailhats, and N. Acar. Comparative study of serine-plasmalogens in human retina and optic nerve: identification of atypical species with odd carbon chains. *J. Lipid Res.* 2012. 53:776–783.

Supplementary key words Eye/retina • mass spectrometry • phospholipids • phospholipids/phosphatidylserine

The nervous system is an organ with the second highest concentration of lipids, only exceeded by adipose tissue. Nervous tissues contain about 50 to 60% of their dry weight as lipids, and approximately 35 to 40% of these lipids are polyunsaturated fatty acids (PUFAs) (1–4). The majority of these lipids appear as PUFA-rich-membrane

phospholipids and cholesterol esters, both playing structural functions without being related to energy metabolism (3). As elements of the nervous system, ocular tissues, such as the optic nerve and the neural retina, display similar composition (5–7). In mammalian cell membranes, phospholipids also comprise ether-linked species containing either an alkyl-ether or a vinyl-ether bond at the *sn*-1 position of glycerol (3, 5, 8). The vinyl-ether-linked species include a carbon-carbon double bond next to the ether linkage in comparison to the ether forms. Vinyl-ether bearing phospholipids are termed as plasmalogens and are found in numerous mammalian cell types, including the retina (9–11), mostly in the forms of phosphatidylcholines (PC) and phosphatidylethanolamines (PE). In plasmalogens, the *sn*-2 position of glycerol backbone is usually occupied by PUFAs, whereas the *sn*-1 position is linked to vinyl-ether moieties with 16 to 18 carbon. The biological functions of plasmalogens are still unclear, although it has been reported that the presence of plasmalogens in membrane affects its fluidity and fusion (8). Due to the high PUFA content of plasmalogens, they are also considered as reservoirs of PUFAs, which can be used by a plasmalogen-specific phospholipase A2 (iPLA2) (12, 13) to liberate free fatty acids in order to be further metabolized into second messenger molecules, such as prostaglandins and thromboxanes (14, 15). The alteration of cellular plasmalogen content has been associated with several human disorders and diseases, such as rhizomelic chondrodysplasia punctata Type 2, Alzheimer's disease, Down syndrome, Zellweger syndrome, and primary open-angle glaucoma (8, 16–18).

Although PC and PE are the major phospholipid classes containing plasmalogens, vinyl-ether bearing phospholipids can also appear in the form of phosphatidylserine (PS).

Abbreviations: PC, phosphatidylcholine; PE, phosphatidylethanolamine; PS, phosphatidylserine.

¹To whom correspondence should be addressed.
e-mail: frederic.destailhats@rdls.nestle.com

Manuscript received 28 November 2011 and in revised form 11 January 2012.

Published, JLR Papers in Press, January 19, 2012

DOI 10.1194/jlr.D022962

Copyright © 2012 by the American Society for Biochemistry and Molecular Biology, Inc.

This article is available online at <http://www.jlr.org>

Recent technical advances, and particularly the development of tandem mass spectrometric methods, have allowed different groups to confirm the presence of PS plasmalogens in bacteria (19), rat lung (19), and in human lens (20) or macrophages (21). PS plasmalogens in the lung and in the lens consist of classical structures with saturated and/or monounsaturated moieties in *sn-1* and *sn-2* positions of the glycerol, whereas PS plasmalogens from macrophages contain PUFA having at least 20 carbon atoms and three double bonds in the *sn-2* position.

The objective of the present work was to identify and compare the apparent abundances of PS plasmalogen species present in human ocular neurons represented by the retina and the optic nerve. By using liquid chromatography coupled to high-resolution and tandem mass spectrometry, we have identified for the first time several species of PS plasmalogens, including atypical forms having moieties with odd numbers of carbons and unsaturation in *sn-2* position. The potential origin and functions of these atypical ether-linked PS in ocular tissues are discussed.

MATERIALS AND METHODS

Chemicals and samples

ULC-grade ammonium-formate, methanol and isopropanol were obtained from Chemie Brunschwig AG, Basel, Switzerland. LC-grade acetone was purchased from Sigma-Aldrich, Buchs, Switzerland. PS standards (16:0-18:1 PS, 18:1 PS, 10:0 PS, 18:0-18:1 PS, 18:2 PS, 16:0-18:2 PS, 16:0-20:4 PS, 16:0-22:6 PS, 18:0-18:2 PS, 18:0-20:4 PS, 18:0-22:6 PS, 20:4 PS, 22:6 PS) were obtained from Avanti Polar Lipids Inc. (Alabaster, AL).

Eyes were collected from six human donors (bodies donated to science, four women and two men, mean age 83.2 ± 17.9 years, range 72–94 years; **Table 1**) within 19 h (median time, mean time 17.9 ± 7 h) after death and were handled in accordance with the guidelines of the Declaration of Helsinki. The bodies were refrigerated at 4°C within 24 h after death. Eyeballs were enucleated at the anatomy laboratory of the Saint Etienne School of Medicine (France). Enucleated eyeballs were immersed in a BSS (Alcon, Rueil Malmaison, France) at 4°C. Within 30 min after enucleation, a circular section at the pars plana was taken with a 18 mm diameter trephine, and the corneoscleral disc was removed for other studies. The posterior pole of the eyeball was placed on a back-lit table, and the retina was observed under an operating microscope to select the tissues further included in this study. No eye having large drusen, severe pigment epithelial alterations,

severe macular atrophy, macular hemorrhage, or grossly visible chorioretinal pathologic abnormality was included in the study. The vitreous body was carefully removed. The entire neural retina ($n = 5$) was carefully separated from the RPE/choroid with forceps. The optic nerves ($n = 5$) were excised by cutting tangential to the sclera after having removed the extraocular tissues. All samples were immediately stored at -80°C until further analyses.

Preparation of standard solutions and samples

PS standards were prepared at $10 \mu\text{g}/\text{mL}$ in methanol:chloroform (9:1). Lipids were extracted from retinas and optic nerves following the Folch's procedure (22). Phospholipids were purified from total lipid extracts using silica cartridges (25×10 mm i.d.; Sep-pak, Waters S.A., Framingham, MA) as previously described (23). Before chromatographic analyses, the phosphorus content of the total phospholipid extract was determined according to the method developed by Bartlett and Lewis (24). The total phospholipid extracts were dried under nitrogen and diluted at a final concentration of $12.5 \text{ ng}/\mu\text{L}$ in chloroform/methanol (1:1, v/v) under argon atmosphere. The extracted solutions were kept at -20°C and were further diluted with methanol 1:1 directly before analysis. Aliquot from this solution ($10 \mu\text{L}$) containing 25% chloroform was injected on the column.

Liquid chromatography

An Accela 1250 liquid chromatograph (ThermoFisher Scientific, Bremen, Germany) equipped with an Agilent Poroshell 120 C18 column (fused-core, $2.7 \mu\text{m}$ particle size, 2.1×150 mm) was used for separation of analytes. The applied gradient is shown in **Table 2**. Solvent A was water enriched with 1% formic acid, solvent B was methanol enriched with 1% formic acid, and solvent C was isopropanol.

Mass spectrometric parameters

An LTQ-Orbitrap XL hybrid mass spectrometer (ThermoFisher Scientific, Bremen, Germany) was used for all high resolution and tandem analyses. Negative electrospray ionization with 3.5 kV capillary voltage was used to form ions at 400°C nebulizer temperature. Nebulizer and auxiliary gases were nitrogen at 40 and 20 units, respectively. Tube lens was adjusted to 80 V. Other parameters were the typical values optimized during calibration. Resolution of 100,000 (full width at half maximum) was applied in the m/z range of 200–1100, and profile data acquisition was performed. A lock mass of m/z 255.23295 was used as a reference point for the internal mass correction. For this purpose, palmitic acid ($100 \text{ mg}/\text{L}$ in methanol) at $50 \mu\text{L}/\text{min}$ was infused into the electrospray assembly via a T-element.

The tandem mass spectrometric experiments were carried out using the collision-induced dissociation fragmentation mode in the linear ion trap. Isolation width was m/z 2, normalized collision

TABLE 1. Characteristics of the human donors

Subject	Gender	Age	Postmortem Delay before Tissue Collection	Collected Tissue
		years	hours	
#1	Female	82	15.0	Retina
#2	Male	72	24.0	Retina, optic nerve
#3	Female	82	7.0	Optic nerve
#4	Male	90	14.0	Retina
#5	Female	94	23.5	Optic nerve
#6	Female	79	24.0	Retina ($\times 2$), optic nerve ($\times 2$)
Mean \pm SD	—	83.2 ± 17.9	17.9 ± 7.0	—
Median	—	82.0	19.3	—
Range	—	72–94	7.0–24.0	—

TABLE 2. Liquid chromatographic gradient applied for the separation of PS plasmalogens. Solvent A was water enriched with 1% formic acid, solvent B was methanol enriched with 1% formic acid, and solvent C was isopropanol

Time	Solvent A	Solvent B	Solvent C	Flow rate
min	%	%	%	$\mu\text{L}/\text{min}$
0	10	90	0	500
3	10	90	0	500
50	0	0	100	350
52.5	0	0	100	350
53	10	90	0	350
55	10	90	0	500
60	10	90	0	500

energy was 35 units, activation Q value was 0.25, and activation time was 30 msec. The software Quanbrowser (ThermoFisher Scientific, Bremen, Germany) was used to generate ion chromatograms in 10 ppm m/z windows at the theoretical m/z channels of PS.

RESULTS

Ionization, chromatography, and fragmentation conditions were optimized using a PS standard mix (10 $\mu\text{g}/\text{ml}$). Negative ion mode proved to be approximately 30 times more sensitive for PS than positive ion mode; therefore, this mode was used in our entire work. In terms of chromatography, the above-described reversed-phase chromatographic conditions were chosen to reduce spectral

complexity, in particular to resolve analyte pairs differing in one double bond. In such cases [e.g., PS(P-18:1/18:1) and PS(P-18:0/18:1)], the required mass resolution would exceed the currently available 100,000; therefore, the isotopomer envelope of the first analyte could not be resolved from the second analyte. An example of such a case is given in Table 3, where the retention time of the potential PS(P-18:1/18:1) is 21 min and that of PS(P-18:0/18:1) is 22.5 min. By using the described chromatographic separation such pairs are sufficiently resolved, enabling their distinct detection and quantification. Furthermore, because phosphatidylserines commonly lose an 87 Da serine fragment independently from the fatty acid chains, the presence of serine moiety in potential PS lipids can be easily confirmed based on the fragmentation pattern.

The preliminary investigations were performed in one representative retina and in one optic nerve sample. These latter were obtained by pooling aliquots from five individual retina and nerve samples. To screen for the potential presence of PS ether-linked species, a list of their theoretical masses was established. The fatty acids 16:0, 16:1, 18:0, 18:1, 20:0, and 20:1 were considered as possible precursors for vinyl chain substituents. The fatty acids 14:0, 16:0, 16:1, 18:0, 18:1, 18:2, 18:3, 18:4, 20:0, 20:1, 20:2, C20:3, 20:4, 20:5, 22:1, 22:3, 22:4, 22:5, and 22:6 were considered as possible ester substituents at the *sn*-2 position. The corresponding pseudomolecular masses ($[M-H]^-$) and the fragments after loss of the serine- and fatty acid residues were also calculated. The theoretical m/z channels in a 10 ppm

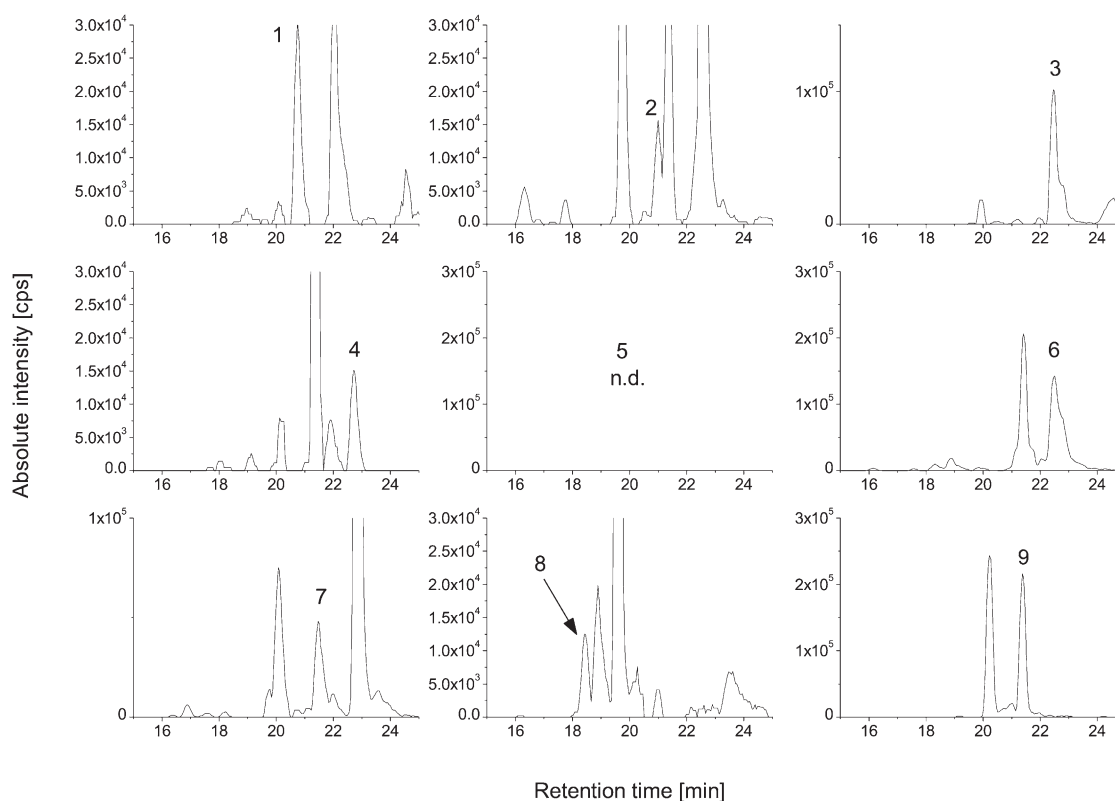


Fig. 1. Ion chromatograms of PS plasmalogens in pooled retina sample. The numeric labels correspond to the PS plasmalogens as given in the tables.

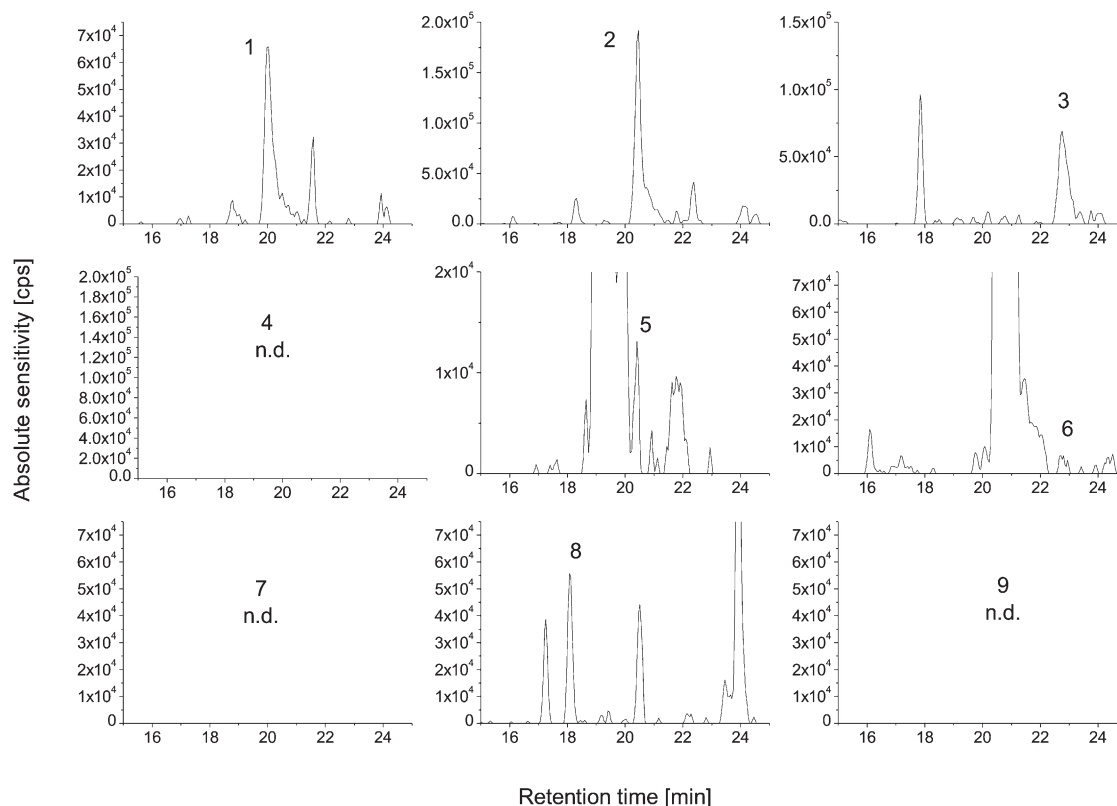


Fig. 2. Ion chromatograms of PS plasmalogens in pooled optic nerve sample. The numeric labels correspond to the PS plasmalogens as given in the tables.

mass window were surveyed for the presence of chromatographic peaks that could correspond to PS ether-linked species. Peaks falling within the mass window and with intensities above 10,000 cps were then subjected to MS/MS analysis as described above. Peaks were considered for further analysis only if they exhibited the characteristic serine loss of 87 Da. Based on this information, the presence of several ether-linked PS was confirmed; see **Figures 1** and **2** and **Tables 3** and **4**, including the observed mass errors. In addition, the chromatographic peak areas obtained from the high-resolution chromatograms were extracted and

were used to compare the apparent abundances of PS plasmalogen species (**Tables 3** and **4**).

Structural elucidation of the potential PS ether-linked species was pursued by performing MS³ experiments: After isolating and fragmenting the [M-H][−] ions, the [M-H-87][−] fragments were again isolated and fragmented. The resulting MS³ fragmentation patterns were then manually interpreted to determine which fatty acids are linked as ether or esters to the glycerol backbone. For this latter purpose, first the fragmentation pattern of the hypothetical PS ether-linked lipids detected in the pooled retina and optic nerve

TABLE 3. PS plasmalogens detected in retina samples

Plasmalogen	Theoretical m/z [M-H] [−]	Observed m/z [M-H] [−]	Mass Error <i>ppm</i>	Retention Time <i>min</i>	Single stage peak area	Peak area, SD <i>%</i>
1 PS(P-16:0/18:1)	744.51849	744.51839	−0.1	20.74	450,209	51
2 PS(P-18:1/18:1)	770.53414	770.53312	−1.3	20.99	241,678	—
3 PS(P-18:0/18:1) and PS(P-16:0/20:1)	772.54979	772.54924	−0.7	22.46	1,943,420	46
4 PS(O-18:0/18:1) and PS(O-16:0/20:1)	774.56544	774.56559	0.2	22.70	293,732	40
5 PS(P-18:1/20:4)	792.51849	n.d.	n.d.	n.d.	n.d.	n.d.
6 PS(P-18:0/20:4) and PS(P-16:0/22:4)	794.53414	794.53159	−3.2	22.50	604,387	41
7 PS(O-18:0/20:4)	796.54979	796.54830	−1.9	21.46	835,972	24
8 PS(P-19:0/20:3) and PS(P-21:2/18:1)	810.56544	810.56522	−0.3	18.41	419,960	31
9 PS(P-19:0/22:3) and PS(P-23:2/18:1)	838.59674	838.59660	−0.2	21.37	3,985,842	21

TABLE 4. PS plasmalogens detected in optic nerve samples

Plasmalogen	Theoretical m/z [M-H] ⁻	Observed m/z [M-H] ⁻	Mass Error <i>ppm</i>	Retention Time <i>min</i>	Single stage peak area	Peak area SD %
1 PS(P-16:0/18:1)	744.51849	744.51823	-0.4	20.03	1,692,272	51
2 PS(P-18:1/18:1)	770.53414	770.53351	-0.8	20.45	2,676,095	49
3 PS(P-18:0/18:1) and PS(P-16:0/20:1)	772.54979	772.54982	0.0	22.75	2,480,154	41
4 PS(O-18:0/18:1) and PS(O-16:0/20:1)	774.56544	n.d.	n.d.	n.d.	n.d.	n.d.
5 PS(P-18:1/20:4)	792.51849	792.51612	-3.0	20.41	1,553,675	36
6 PS(P-18:0/20:4) and PS(P-16:0/22:4)	794.53414	794.53153	-3.3	22.80	775,297	10
7 PS(O-18:0/20:4)	796.54979	n.d.	n.d.	n.d.	n.d.	n.d.
8 PS(P-19:0/20:3) and PS(P-21:2/18:1)	810.56544	810.56464	-1.0	18.69	630,822	30
9 PS(P-19:0/22:3) and PS(P-23:2/18:1)	838.59674	n.d.	n.d.	n.d.	n.d.	n.d.

samples were studied in detail. Based on this, three fragments were proposed as marker ions to deduce which fatty acid is linked as ether or ester on the glycerol backbone (Fig. 3). Interpretation of the fragmentation patterns according to this scheme enabled the assignment of structures to the m/z values to identify the PS plasmalogens. An example MS³ fragmentation pattern is shown in Fig. 4, which depicts the obtained fragments after isolating and fragmenting first the [M-H]⁻ ions then isolating and fragmenting the [M-H-87]⁻ ions. This methodology does not allow distinction between isomers of fatty acids (e.g., straight vs. branched chains).

After the various PS plasmalogen species were detected and identified, they were analyzed in the individual samples (5 retinas + 5 optic nerves). The averaged peak areas with the observed mass errors and retention times are given in Tables 3 and in 4. The results are also shown in Fig. 5.

DISCUSSION

Our data show that retinal and optic nerve PS plasmalogens consisted of typical structures found in other tissues, such as PS(P-18:0/18:1), PS(P-18:1/18:1), and PS(P-18:0/18:1) + PS(P-16:0/20:1). Except for PS(P-18:0/18:1) + PS(P-16:0/20:1), these species were found at higher abundance in the optic nerve when compared with the retina. This disparity is consistent with evidences showing that *i*) the optic nerve is composed of myelinated axons (25) and *ii*) serine phospholipid chains in myelin contain high levels of saturated and monounsaturated 18-carbon chains (26).

A striking difference was observed between the retina and the optic nerve concerning the PS species esterified with arachidonic (20:4 n-6) acid. The profiles of these two ocular tissues were quite different because the optic nerve was characterized by a high level of PS(P-18:1/20:4),

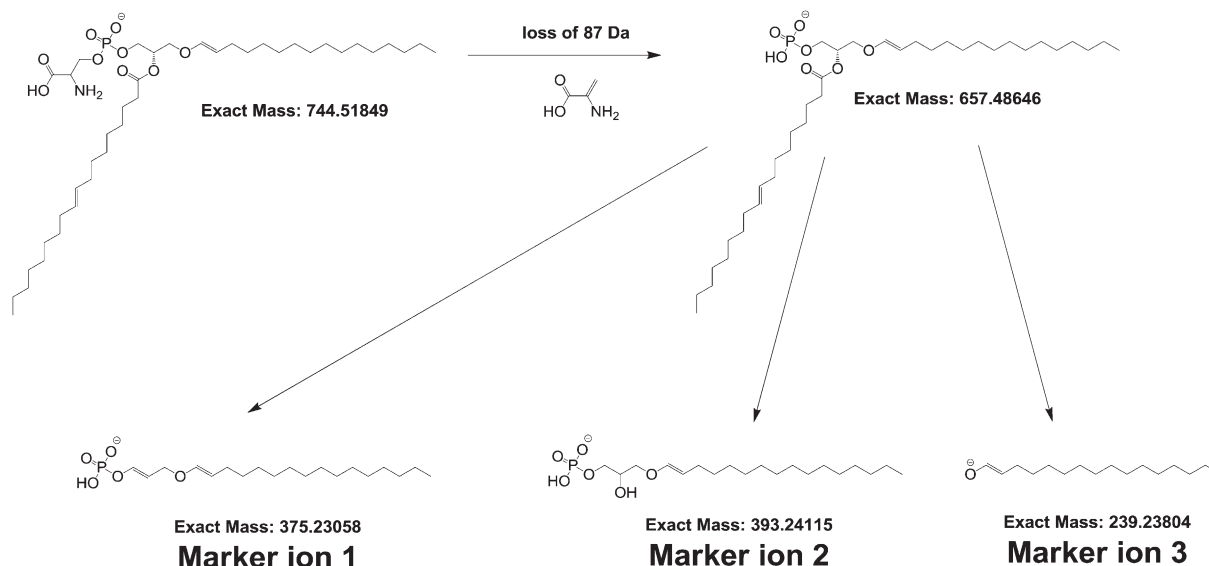


Fig. 3. Proposed collision-induced dissociation fragmentation pathway of PS plasmalogens. After the loss of the 87 Da unit reflecting the presence of serine moiety, three marker ions are postulated. These ions enable us to deduce which fatty acid is linked as ether or ester to the glycerol backbone.

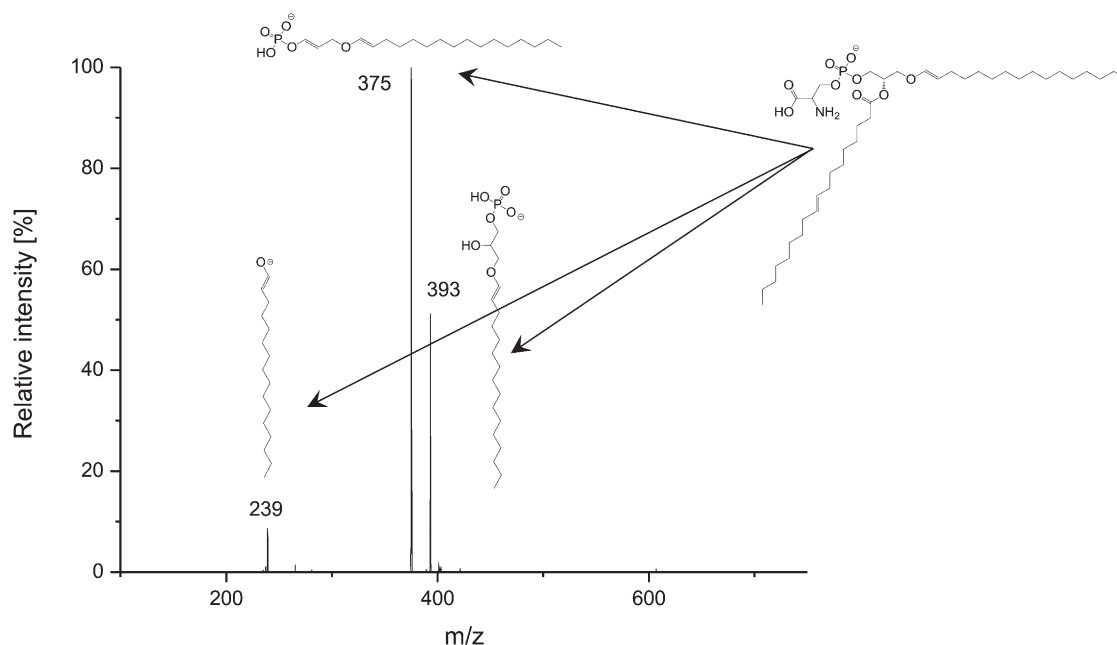


Fig. 4. MS³ fragmentation pattern of PS (P-16:0/18:1). Note the presence of the three marker ions and their accordance with Figure 1.

whereas this compound was not detected in the retina. Considering the various metabolic pathways of arachidonic acid in neurons (27), the functions played by this particular PS plasmalogen might be specific to these tissues and related to eicosanoid metabolism. On the contrary, other PS species, namely PS(O-18:0/20:4) and PS(O-18:0/18:1) + PS(O-16:0/20:1), were found in the retina but not in the optic nerve. Because the optic nerve is exclusively composed of myelinated axons, and subsequently comparable to the brain tissue, our data are consistent with previous studies revealing higher concentration of saturated phospholipids in the retina when compared with cerebral neurons (28). The functional implication of retinal PS plasmalogen species is unknown, but the above-mentioned biochemical particularity of retinal tissue may be the result of a relatively low activity of alkyl-acyl phosphoglyceride desaturase, which catalyzes the conversion of

alkyl-ether phospholipids into vinyl-ether phospholipids (29). Further, while the presence of PS lipids on the outer leaflet of the plasma membrane is a well established marker of apoptosis, to our knowledge, the affinity of PS binding proteins, such as Annexin V, for ether-linked PS species has not been tested (30). Following the identification of these species in multiple tissues, it would be interesting to pursue this further.

During the analysis of human retinas and optic nerves, we have also identified PS(P-19:0/20:3) + PS(P-21:2/18:1) and PS(P-19:0/22:3) + PS(P-23:2/18:1) (Tables 3 and 4; Fig. 5). To our knowledge, none of the previous works on human tissues have shown the existence of species having at least one odd carbon fatty acid. Interestingly, PS(P-19:0/20:3) + PS(P-21:2/18:1) was exclusively detected in the retina and at a high proportion, suggesting a particular function in this tissue.

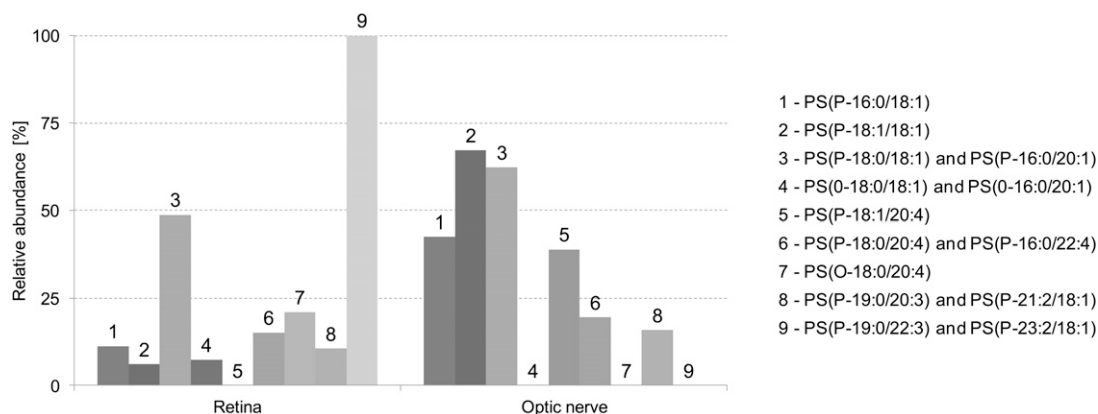



Fig. 5. Relative abundance of PS plasmalogens in retina and optic nerve samples. The bars represent averaged results of the individual analyses. For deviation among the samples, see Tables 3 and 4.

Although it is well established that even-numbered fatty acids are predominant in vertebrates, odd-numbered fatty acids have been also identified in various forms (e.g., sphingolipids, triglycerides, and glycerophospholipids) in numerous tissues, such as the testes, skin, and cataract tissue (31, 32). These fatty acids can enter the food chain via synthesis by ruminant bacteria and plants (31, 33). However, even in the absence of odd-chain fatty acids in the animal diet, they have been identified in significant amounts in the sphingomyelin pool (34), and Nakano et al. (35) have shown that in rat the shorter-, odd-chain fatty acids might also get elongated by the liver. These findings suggest that a mechanism may exist by which the detected odd-chain fatty acids may be synthesized in mammals. One such mechanism could be via α oxidation of fatty acids. Apart from that, disorders of propionate catabolism (such as propionic acidemia) result in increased concentrations of odd-chain fatty acid in the plasma (36). This suggests that propionic acid can be used by mammalian systems to generate odd-chain fatty acids. However, because the retinal tissue we analyzed was collected from elderly donors, these genetic disorders are highly unlikely as the cause of significant presence of odd chain fatty acids. Instead, because a vitamin B12 deficiency state has also been suggested to increase odd-chain fatty acids, we believe this to be a more likely explanation (36, 37).

Because the overall abundance of the above-mentioned odd carbon number fatty acids in the *sn*-1 esterified PS, PC, and PE pool was not determined, the biological significance of this finding needs to be investigated further. Considering the existence of a plasmalogen-specific phospholipase A2 (iPLA2) (12, 13) and the higher metabolic responsiveness and activity of retinal neurons when compared with those from the optic nerve, one can suggest the implication of PS (P-19:0/20:3) + PS (P-21:2/18:1) in cellular signaling after a release from cell membranes, followed by a possible metabolism into second messengers. Furthermore, as shown by several studies conducted in rats and human patients with metabolic diseases, other functions of odd carbon fatty acids in cells could be related to energy production (38–40).

CONCLUSIONS

In summary, this study confirms the presence of various PS plasmalogen species in optic nerve and retina. The results revealed substantial differences in the abundance of these species in these samples, reflecting the structural origin and functional difference between these two tissues. We also confirmed the presence of odd-chain fatty acids in the PS plasmalogen species; however, the biological significance of this latter finding needs to be further investigated. 

The authors thank Pr Gilles Thuret and Pr Philippe Gain (Faculty of Medicine, Laboratory of Biology, Engineering and Imaging of Corneal Graft at Saint-Etienne, France) for collecting and providing retinas and optic nerves from human donors and

Stéphane Grégoire, Lucy Martine, and Stéphanie Cabaret (Centre des Sciences du Goût et de l'Alimentation, Dijon, France) for preparing the samples prior to liquid chromatography.

REFERENCES

- Martinez, M. 1992. Tissue levels of polyunsaturated fatty acids during early human development. *J. Pediatr.* **120**: S129–S138.
- Martinez, M., A. Ballabriga, and J. J. Gil-Gibernau. 1988. Lipids of the developing human retina: I. Total fatty acids, plasmalogens, and fatty acid composition of ethanolamine and choline phosphoglycerides. *J. Neurosci. Res.* **20**: 484–490.
- Sastry, P. S. 1985. Lipids of nervous tissue: composition and metabolism. *Prog. Lipid Res.* **24**: 69–176.
- Makrides, M., M. A. Neumann, R. W. Byard, K. Simmer, and R. A. Gibson. 1994. Fatty acid composition of brain, retina, and erythrocytes in breast- and formula-fed infants. *Am. J. Clin. Nutr.* **60**: 189–194.
- Das, S. K., M. E. Steen, M. S. McCullough, and D. K. Bhattacharyya. 1978. Composition of lipids of bovine optic nerve. *Lipids.* **13**: 679–684.
- Greiner, C. A., J. V. Greiner, C. D. Leahy, D. B. Auerbach, M. D. Marcus, L. H. Davies, W. Rodriguez, and T. Glonek. 1995. Distribution of membrane phospholipids in the rabbit neural retina, optic nerve head and optic nerve. *Int. J. Biochem. Cell Biol.* **27**: 21–28.
- Fliesler, S. J., and R. E. Anderson. 1983. Chemistry and metabolism of lipids in the vertebrate retina. *Prog. Lipid Res.* **22**: 79–131.
- Nagan, N., and R. A. Zoeller. 2001. Plasmalogens: biosynthesis and functions. *Prog. Lipid Res.* **40**: 199–229.
- Acar, N., S. Gregoire, A. Andre, P. Juaneda, C. Joffre, A. M. Bron, C. P. Creuzot-Garcher, and L. Bretillon. 2007. Plasmalogens in the retina: in situ hybridization of dihydroxyacetone phosphate acyltransferase (DHAP-AT)—the first enzyme involved in their biosynthesis—and comparative study of retinal and retinal pigment epithelial lipid composition. *Exp. Eye Res.* **84**: 143–151.
- Berdeaux, O., P. Juaneda, L. Martine, S. Cabaret, L. Bretillon, and N. Acar. 2010. Identification and quantification of phosphatidylcholines containing very long chain polyunsaturated fatty acid (VLC-PUFA) in bovine and human retina by liquid chromatography/tandem mass spectrometry. *J. Chromatogr. A.* **1217**: 7738–7748.
- Bretillon, L., G. Thuret, S. Gregoire, N. Acar, C. Joffre, A. M. Bron, P. Gain, and C. P. Creuzot-Garcher. 2008. Lipid and fatty acid profile of the retina, retinal pigment epithelium/choroid, and the lacrimal gland, and associations with adipose tissue fatty acids in human subjects. *Exp. Eye Res.* **87**: 521–528.
- Hazen, S. L., R. J. Stuppy, and R. W. Gross. 1990. Purification and characterization of canine myocardial cytosolic phospholipase A2. A calcium-independent phospholipase with absolute fl-2 regioselectivity for diradyl glycerophospholipids. *J. Biol. Chem.* **265**: 10622–10630.
- Portilla, D., and G. Dai. 1996. Purification of a novel calcium-independent phospholipase A2 from rabbit kidney. *J. Biol. Chem.* **271**: 15451–15457.
- Fonteh, A. N., and F. H. Chilton. 1992. Rapid remodeling of arachidonate from phosphatidylcholine to phosphatidylethanolamine pools during mast cell activation. *J. Immunol.* **148**: 1784–1791.
- Gaposhkin, D. P., H. W. Farber, and R. A. Zoeller. 2008. On the importance of plasmalogen status in stimulated arachidonic acid release in the macrophage cell line RAW 264.7. *Biochim. Biophys. Acta.* **1781**: 213–219.
- Brites, P., H. R. Waterham, and R. J. Wanders. 2004. Functions and biosynthesis of plasmalogens in health and disease. *Biochim. Biophys. Acta.* **1636**: 219–231.
- Gorgas, K., A. Teigler, D. Komljenovic, and W. W. Just. 2006. The ether lipid-deficient mouse: tracking down plasmalogen functions. *Biochim. Biophys. Acta.* **1763**: 1511–1526.
- Acar, N., O. Berdeaux, P. Juaneda, S. Gregoire, S. Cabaret, C. Joffre, C. P. Creuzot-Garcher, L. Bretillon, and A. M. Bron. 2009. Red blood cell plasmalogens and docosahexaenoic acid are independently reduced in primary open-angle glaucoma. *Exp. Eye Res.* **89**: 840–853.
- Kaneshiro, E. S., Z. Guo, D. Sul, K. A. Kallam, K. Jayasimhulu, and D. H. Beach. 1998. Characterizations of *Pneumocystis carinii* and rat lung lipids: glyceryl ethers and fatty alcohols. *J. Lipid Res.* **39**: 1907–1917.

20. Deeley, J. M., M. C. Thomas, R. J. Truscott, T. W. Mitchell, and S. J. Blanksby. 2009. Identification of abundant alkyl ether glycerophospholipids in the human lens by tandem mass spectrometry techniques. *Anal. Chem.* **81**: 1920–1930.
21. Ivanova, P. T., S. B. Milne, and H. A. Brown. 2010. Identification of atypical ether-linked glycerophospholipid species in macrophages by mass spectrometry. *J. Lipid Res.* **51**: 1581–1590.
22. Folch, J., M. Lees, and G. H. Sloane Stanley. 1957. A simple method for the isolation and purification of total lipids from animal tissues. *J. Biol. Chem.* **226**: 497–509.
23. Juaneda, P., and G. Rocquelin. 1985. Rapid and convenient separation of phospholipids and non phosphorus lipids from rat heart using silica cartridges. *Lipids.* **20**: 40–41.
24. Bartlett, E. M., and D. H. Lewis. 1970. Spectrophotometric determination of phosphate esters in the presence and absence of orthophosphate. *Anal. Biochem.* **36**: 159–167.
25. Huizing, M., B. P. Brooks, and Y. Anikster. 2005. Optic atrophies in metabolic disorders. *Mol. Genet. Metab.* **86**: 51–60.
26. MacBrinn, M. C., and J. S. O'Brien. 1969. Lipid composition of optic nerve myelin. *J. Neurochem.* **16**: 7–12.
27. Bosetti, F. 2007. Arachidonic acid metabolism in brain physiology and pathology: lessons from genetically altered mouse models. *J. Neurochem.* **102**: 577–586.
28. Dorman, R. V., A. D. Toews, and L. A. Horrocks. 1977. Plasmalogenase activities in neuronal perikarya, astroglia, and oligodendroglia isolated from bovine brain. *J. Lipid Res.* **18**: 115–117.
29. Paltauf, F., and A. Holasek. 1973. Enzymatic synthesis of plasmalogens. Characterization of the 1-O-alkyl-2-acyl-8n-glycero-3-phosphorylethanolamine desaturase from mucosa of hamster small intestine. *J. Biol. Chem.* **248**: 1609–1615.
30. Schutters, K., and C. Reutelingsperger. 2010. Phosphatidylserine targeting for diagnosis and treatment of human diseases. *Apoptosis.* **15**: 1072–1082.
31. Rezanka, T., and K. Sigler. 2009. Odd-numbered very-long-chain fatty acids from the microbial, animal and plant kingdoms. *Prog. Lipid Res.* **48**: 206–238.
32. Tao, R. V., B. C. Lee, T. C. Hsieh, and R. A. Laine. 1987. Occurrence of an unusual amount of an odd-numbered fatty acid in glycosphingolipids from human cataracts. *Curr. Eye Res.* **6**: 1361–1367.
33. Or-Rashid, M. M., M. Odongo, N. E. Mc, and B. W. Bride. 2007. Fatty acid composition of ruminal bacteria and protozoa, with emphasis on conjugated linoleic acid, vaccenic acid, and odd-chain and branched-chain fatty acids. *J. Anim. Sci.* **85**: 1228–1234.
34. Bettger, W. J., and C. B. Blackadar. 1997. Dietary very long chain fatty acids directly influence the ratio of tetracosenoic (24:1) to tetracosanoic (24:0) acids of sphingomyelin in rat liver. *Lipids.* **32**: 51–55.
35. Nakano, N., N. Shirasaka, H. Koyama, M. Hino, T. Murakami, S. Shimizu, and H. Yoshizumi. 2000. C19 odd-chain polyunsaturated fatty acids (PUFAs) are metabolized to C21-PUFAs in a rat liver cell line, and curcumin, gallic acid, and their related compounds inhibit their desaturation. *Biosci. Biotechnol. Biochem.* **64**: 1641–1650.
36. Coker, M., J. B. de Klerk, B. T. Poll-The, J. G. Huijman, and M. Duran. 1996. Plasma total odd-chain fatty acids in the monitoring of disorders of propionate, methylmalonate and biotin metabolism. *J. Inher. Metab. Dis.* **19**: 743–751.
37. Metz, J. 1992. Cobalamin deficiency and the pathogenesis of nervous system disease. *Annu. Rev. Nutr.* **12**: 59–79.
38. Gu, L., G. F. Zhang, R. S. Kombu, F. Allen, G. Kutz, W. U. Brewer, C. R. Roe, and H. Brunengraber. 2010. Parenteral and enteral metabolism of anaplerotic triheptanoin in normal rats. II. Effects on lipolysis, glucose production, and liver acyl-CoA profile. *Am. J. Physiol. Endocrinol. Metab.* **298**: E362–E371.
39. Kinman, R. P., T. Kasumov, K. A. Jobbins, K. R. Thomas, J. E. Adams, L. N. Brunengraber, G. Kutz, W. U. Brewer, C. R. Roe, and H. Brunengraber. 2006. Parenteral and enteral metabolism of anaplerotic triheptanoin in normal rats. *Am. J. Physiol. Endocrinol. Metab.* **291**: E860–E866.
40. Roe, C. R., L. Sweetman, D. S. Roe, F. David, and H. Brunengraber. 2002. Treatment of cardiomyopathy and rhabdomyolysis in long-chain fat oxidation disorders using an anaplerotic odd-chain triglyceride. *J. Clin. Invest.* **110**: 259–269.